DOI: https://doi.org/10.26682/sjuod.2020.23.2.6
Journal of University of Duhok, Vol. 23, No.2 (Pure and Eng. Sciences), Pp 49-58, 2020

OPTIMUM LOCATION OF SPVG TO ENHANCE VOLTAGE STABILITY USING STATIC TECHNIQUES

MELAT **K**. **A**BDULLA and **L**OKMAN **H**. **H**ASSAN
Dept. of Electrical and Computer Engineering, College of Engineering, University of Duhok, Kurdistan Region-Iraq

(Received: May 5, 2020; Accepted for Publication: June 30, 2020)

ABSTRACT

Solar Photovoltaic Generators (SPVGs) play a great and vital role in providing clean and enough energy to meet power loads. However, SPVGs integration on power systems increase power grid problems. It will lead to different problems including disturbance of the grid, instability of the voltage and swings of the power. The impact of SPVG on the voltage stability of the system is studied in this paper. The best location of SPVG is obtained using three static techniques. Power flow and the Q-V curve techniques are used to identify the weakest buses and test the stability of the system under nominal load condition respectively. On other hand, Continuation Power Flow (CPF) and the Q-V curve techniques are used to identify the weakest buses and test the stability of the system under heavy load condition respectively. The proposed techniques are apllied to the New England 39-bus standard system under various loading conditions. The results reveal that choosing a proper location for the SPVG will improve the voltage stability of the system. In addition, connecting the SPVG at the nearest bus to the weakest bus provides better performance than when it connected to the weakest bus.

KEYWORDS:

1. INTRODUCTION

Voltage stability is the capability of a power grid at a specified initial working state to keep on steady voltages at all buses of the network under a disturbance. When voltage instability causes a very low voltage in an important part of the network and consequently results in partial or total blackout known as voltage collapse (Kundur et al., 2004; Vahid-Pakdel, Seyedi, & Mohammadi-Ivatloo, 2018).

Renewable energy sources, such as Solar Photovoltaic Generators (SPVGs), play a considerable role in providing clean energy and generating a suitable supply to meet an energy request. PV generators can be used to deliver reactive power support to the network. However, integrating SPVG into a grid can affect the stability of the grid (Omole, 2010). Therefore, the voltage stability should be considered when the SPVG generators are joined to the network.

Dynamic and static are two methods that used in the literature to analyse the voltage stability of the system.

Dynamic analysis techniques were used in (Noel, Sozinho, Wilson, & Hatipoglu, 2016; Refaat, Abu-Rub, Sanfilippo, & Mohamed, 2018) to prove that the photovoltaic system can support the system the power needs. Hassan (Lokman H. Hassan, 2017) presented a full dynamic analysis of voltage stability effect on the IEEE 69-bus and IEEE 118-bus distribution systems with PV generators. In (Munkhchuluun & Meegahapola, 2017), an improvement of the long term voltage stability of the system was occurred after adding the SPVG to the Nordic-32 bus system using time-domain simulation. However, dynamic analysis approaches are time-consuming and need burden computation.

Static methods are usually used for analysing the stability of the voltage due to their simplicity and reasonable accuracy (Lokman H. Hassan, Mohamed, Moghavvemi, & Yang, 2008). In (Y.-B. Wang, Wu, Liao, & Xu, 2008), the steady-state characteristics of the PV emerging into a power system was studied using only the power flow technique. The performance and modelling SPVG on voltage stability were conducted in (Tamimi, Cañizares, & Bhattacharya, 2011) and (Tamimi, Canizares, & Bhattacharya, 2013) using 14-bus with three generators test system and the Ontario test system as case studies respectively. In both researches, only the Continuation Power Flow (CPF) technique was used. The inclusion of SPVG improved the system stability by increasing the loadability

melatsharafany89@gmail.com

boundary. In (Chang et al., 2015), the impact of PV generator on system capacity at two system points was studied by using only power flow technique. In (Nikpour, 2016), static and dynamic voltage stability studies were carried out for distribution systems with distributed generation using a voltage stability index and shifted frequency analysis respectively. It presents that adding PV to a system, the percentage of general system capacity increases. CPF analysis is applied in (Suampun, 2016) for investigating the stability of the voltage of net-connected PV power grids under heavy load condition. In (Xue, Manjrekar, Lin, Tamayo, & Jiang, 2011), a study on the transient and static voltage characteristics at the connecting point of the PV to a system was presented using P-V curve technique. In (A. Elrheem E.A. Mostafa, Naglaa K. Bahgaat, Mohamed Ebrahim El sayed, & Othman4, 2017), the genetic algorithm procedure was used to tune the PI controller of the SPVG for enhancing voltage stability. Q-V curve technique was used by D. Wang et al. (D. Wang, Yuan, Zhao, & Qian, 2017) to show the impact of the SPVG on the static voltage stability of the China's Qinghai network. The IEEE 34 node test feeder was used in (Ghaffarianfar & Hajizadeh, 2018) to investigate the impact of PV penetration on the voltage stability of distribution systems. In (Sinder, Assis, & Taranto, 2019), the effect of the SPVG on voltage stability margin in an islanded micro grid was studied. The P-V curve analysis was applied in the last two papers. From the literature review, it is clear that the impact of the SPVG on the voltage stability was studied using only one of the static techniques.

In this paper, a comprehensive study is carried out to demonstrate the impact of the SPVG in improving the voltage stability of power systems by using three static techniques (i.e. power flow, Q-V curve and CPF). The proposed techniques are tested on the New England 39-bus standard system under nominal and heavy load conditions.

The rest of the paper is arranged as follows: Section 2 presents modelling of the solar photo-voltaic generation. In Section 3, three static analysis techniques for voltage stability are described. Simulation results and discussion are presented in Section 4. Finally, the conclusion of the paper is given in section 5.

2. MODELLING OF THE SOLAR PHOTO-VOLTAIC GENERATION

Fig. (1 shows the characteristic structure of a network connected to a photovoltaic generator.

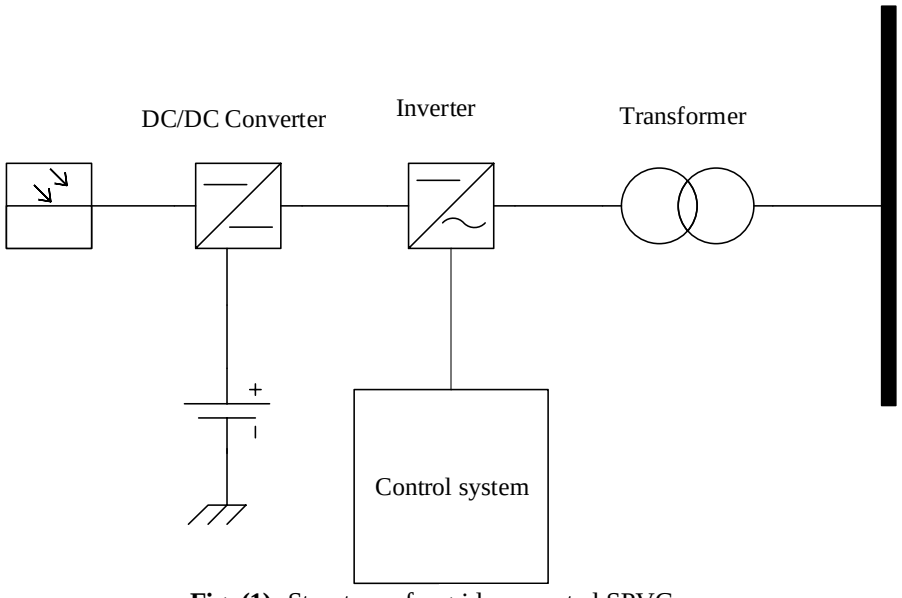

Fig. (1): Structure of a grid-connected SPVG

melatsharafany89@gmail.com

The SPVG consists of photovoltaic arrays, a DC/DC converter and an inverter. The outputs of the inverter are [6]:

$$i_d = \frac{1}{1+sT_p} i_{d\,s} \quad (1)$$

$$i_q = \frac{1}{1+sT_q} i_{q\,s} \quad (2)$$

where: i_d , i_q the output currents of the inverter; T_p , T_q The steady-state gains and $i_{d\,s}$, $i_{q\,s}$ are the currents set-point.

The set-point currents can be calculated depending on the chosen active power and reactive powers as:

$$\begin{bmatrix} i_{d\,s} \\ i_{q\,s} \end{bmatrix} = \begin{bmatrix} v_d & v_q \\ v_q & -v_d \end{bmatrix}^{-1} \begin{bmatrix} P \\ Q \end{bmatrix} \quad (3)$$

The value of the reactive power reference is calculated depending on the value of the actual and set-point voltage through the PI controller as:

$$Q = (k_v + k_i s)(v_{dc} - v_{dc\,ref}) \quad (4)$$

3. VOLTAGE STABILITY ANALYSIS

In this section, three static analysis techniques for voltage stability are described. These techniques are used to measure the stability of the voltage of the grid under different conditions. These techniques are power flow, Q-V cure and continuous power flow.

3.1 Power flow analysis

The electric utility industry widely depends on power flow as a static analysis to assess the voltage stability. The power flow analysis is used to calculate the power flow via transmission line and voltage for buses or specific terminals. The system equations in term of the bus admittance matrix can be written as (Kundur, 1994):

$$\begin{bmatrix} \vec{I}_1 \\ \vec{I}_2 \\ \vdots \\ \vec{I}_n \end{bmatrix} = \begin{bmatrix} Y_{11} & Y_{12} & \dots & Y_{1n} \\ Y_{21} & Y_{22} & \dots & Y_{2n} \\ \vdots & \vdots & \vdots & \vdots \\ Y_{n1} & Y_{n2} & \dots & Y_{nn} \end{bmatrix} \begin{bmatrix} \vec{V}_1 \\ \vec{V}_2 \\ \vdots \\ \vec{V}_n \end{bmatrix} \quad (5)$$

where Y is admittance and n is number of buses

The current at any bus is related to active power, reactive power and voltage as:

$$\vec{I}_b = \frac{P_b - jQ_b}{\overrightarrow{V^*}_b} \quad (6)$$

where P is active power, Q is reactive power and b is bus number.

$$\vec{I}_b = \sum_{m=1}^{n} \vec{Y}_{bm}\ \vec{V}_m \quad (7)$$

Then

$$P_b + JQ_b = \vec{V}_b \sum_{m=1}^{n} (G_{bm} - JB_{bm})\,\overrightarrow{V^*}_m \quad (8)$$

where G is conductance, B is susceptance and $Y = G \pm jB$.

The product of phases of $\vec{V}_b$ and $\overrightarrow{V^*}_m$ can be written as:

$$\begin{aligned} \vec{V}_b\,\overrightarrow{V^*}_m &= \left(V_b e^{i\theta_b}\right)\left(V_m e^{-i\theta_m}\right) \\ &= V_b\,V_m e^{i(\theta_b - \theta_m)} \\ &= V_b\,V_m(\cos\theta_{bm} + j\sin\theta_{bm}) \end{aligned} \quad (9)$$

where $\theta_{bm} = \theta_b - \theta_m$ is the phase from bus to bus

Then the active and reactive powers at each bus are the function of voltage magnitude and phase angle as:

$$P_b = V_b \sum_{m=1}^{n} (G_{bm}V_m \cos\theta_{bm} + B_{bm}V_m \sin\theta_{bm}) \quad (10)$$

$$Q_b = V_b \sum_{m=1}^{n} (G_{bm}V_m \sin\theta_{bm} - B_{bm}V_m \cos\theta_{bm}) \quad (11)$$

3.2 Q–V modal analysis

Voltage is fully associated with reactive powerby assuming real power at every operating point is constant. Then the stability of the voltage can be calculated via the incremental relation between reactive power and voltage (Heetun, Abdel Aleem, & Zobaa, 2016). The reduced Jacobian matrix is given as:

$$\Delta Q = J\Delta V \quad (12)$$

Furthermore, Jacobian matrix may be factored as:

$$J = x\Lambda^{-1}\eta \quad (13)$$

where x is the right eigenvector matrix of Jacobian matrix, Λ is the diagonal eigenvector matrix of Jacobian matrix and η is the left eigenvector matrix of Jacobian matrix.

The variation of voltage against the reactive power is:

$$\Delta V = x\Lambda^{-1}\eta\Delta Q \quad (14)$$

$$\Delta V = \sum_i (x_i\eta_i/\lambda_i)\Delta Q \quad (15)$$

where x_i is the ith column of the right eigenvalue of Jacobian matrix, η_i is the ith row

melatsharafany89@gmail.com

of the left eigenvalue of Jacobian matrix and λ_i is the ith eigenvalue of Jacobian matrix got from the diagonal matrix(Λ^{-1}).

The voltage deviation for the *i*-th mode is obtained as:

$$V_i = \frac{1}{\lambda_i}\, q_i \tag{16}$$

Eigenvalues of the Jacobian matrix are utilized as an indication for the voltage stability of the system. The grid is stable when all the eigenvalues have positive value. Otherwise, the grid is unstable when minimum eigenvalue is equal to zero or less than zero. Therefore, the minimum value of positive eigenvalue, the nearer the system is to voltage instability. the V–Q sensitivity at b bus is driven as:

$$\frac{\partial V_b}{\partial Q_b} = \sum_i \frac{x_{bi}\, \eta_{bi}}{\lambda_i} \tag{17}$$

When the Q-V sensitivity is negative, this involves that the grid is unstable. The lesser the sensitivity, the more stable is the grid. In order to obtain the relation between the system buses and each eigenvalue, the participation factor is considered as:

$$P_{bi} = x_{bi}\, \eta_{bi} \tag{18}$$

4.3 Continuous power flow analysis

The continuation technique is a calculated path-following calculation procedure that used to calculate nonlinear equations for the system (A. D. Vasquez & T. Sousa, 2017). From the Newton-Raphson, load flow equations can be driven by introducing a load parameter into equations as:

$$P_b - \sum_{m=1}^{n} Y_{bm} V_b\, V_m \cos(\theta_{bm}) = 0 \tag{19}$$

$$Q_b - \sum_{m=1}^{n} Y_{bm} V_b\, V_m \sin(\theta_{bm}) = 0 \tag{20}$$

Let λ is load factor:

$$P_{Lb} = P_{L0} + \lambda(R_{Lb} S_{base}\ cos\,\theta_b) \tag{21}$$

$$Q_{Lb} = Q_{L0} + \lambda(R_{Lb} S_{base}\ sin\,\theta_b) \tag{22}$$

where P_{L0} and Q_{L0} are nominal active and reactive load at bus b, R_{Lb} is a multiplier to show the amount of load change at bus b as load factor (λ) changes and S_{base} is a given amount of apparent power which is selected to provide suitable value of λ.

The equations of power flow maybe written as:

$$F(\theta, v, \lambda) = 0 \tag{23}$$

where θ represents the vector of bus voltage angles and v represents the vector of bus voltage magnitudes.

The active power generation term is adjusted as:

$$P_{Gb} = P_{G0}(1 + \lambda R_{Gb}) \tag{24}$$

where P_{Gb} is the active power generation at bus b; P_{G0} is the initial value of active power generation; R_{Gb} is the constant of varying rate in generation to resolve the problem.

A linear estimate technique is utilized by selecting a suitable step size in a direction tangent to the resolution path. Then (23) is derived as:

$$F_\theta d\theta + F_v dv + F_\lambda d\lambda = [F_\theta\ F_v\ F_\lambda] \begin{bmatrix} d\theta \\ dv \\ d\lambda \end{bmatrix} = 0 \tag{25}$$

After adding λ to load flow equations, an additional equation is required to solve (25). This will be carried out by assuming one of the tangent vector components equal to +1 or -1, which is known as parameter of the continuation.

$$\begin{bmatrix} F_\theta\ F_v\ F_\lambda \\ e_b \end{bmatrix} \begin{bmatrix} d\theta \\ dv \\ d\lambda \end{bmatrix} = \begin{bmatrix} 0 \\ \pm 1 \end{bmatrix} \tag{26}$$

where e_b is the suitable row vector with entirely elements equal to zero excluding the b^{th} element equals to 1.

First, λ is selected as the continuation parameter and as the process is continued the state variable with the highest amount of change is chosen as continuation parameter because of nature of parameterization. By solving (26), the tangent vector is obtained. The prediction is:

$$\begin{bmatrix} \theta \\ v \\ \lambda \end{bmatrix}^{p+1} = \begin{bmatrix} \theta \\ v \\ \lambda \end{bmatrix}^{p} + \sigma \begin{bmatrix} d\theta \\ dv \\ d\lambda \end{bmatrix} \tag{27}$$

where the next step is designated by $p + 1$ and the step size σ is selected so the estimated solution is within the radius of the corrector convergence.

The predicted result is adjusted via local parameterization. The equation (26) is improved by using one equation that identifies the amount of state variable selected as:

$$\begin{bmatrix} F(\theta, v, \lambda) \\ x_b - \eta \end{bmatrix} = 0 \tag{28}$$

where x_b is state variable selected as continuation parameter and η is the predicted value of the state variable.

4. RESULTS AND DISCUSSIONS

New England 39-bus system is used as the test system. Data of the system are given in (L.

melatsharafany89@gmail.com

Hassan, Moghavvemi, & Almurib, 2012). The single line diagram of the sysem is shown in the Appendix. The study is carried out using Power System Analysis Toolbox (PSAT) which is a MATLAB based toolbox for power system studies.

4.1 The weakest bus

To identify the weakest buses of the system, power flow and the Q-V curve are used for nominal condition and continues power flow with the Q-V curve are used for heavy load condition. Also the total power system losses is calculated in both conditions.

4.1.1 Nominal load condition

Table (1 demonstrates three weakest buses based on the power flow results.

Table (1): Power flow result

Bus	V p.u.	Phase rad.	P_g p.u.	Q_g p.u.	P_L p.u.	Q_L p.u.
Bus 32	0.93491	-0.11367	0	0	0.075	0.88
Bus 17	0.94407	-0.18854	0	0	2.338	0.84
Bus 18	0.94479	-0.19837	0	0	5.220	1.76

The weakest buses are bus 32 with voltage 0.93491 pu then followed by bus 17 and bus 18 with voltages 0.94407 pu and 0.94479 pu, respectively.

By using Q-V curve technique, eigenvalue of each bus is calculated and listed in Table 2.

Table (2): Eigenvalue of weakest buses

Bus	Eigenvalue
Bus 32	38
Bus 17	290
Bus 18	343

The results show bus 32 is the weakest bus of the system because it has the lowest eigenvalue which is equal to 38.

4.1.2 Heavy load condition

Table 3): demonstrates ten weakest buses according to the CPF results.

Table 3 CPF results

Bus	V p.u.	Phase rad.	P_g p.u.	Q_g p.u.	P_L p.u.	Q_L p.u.
Bus 17	0.58128	-0.84679	0	0	4.9133	1.7653
Bus 18	0.58496	-0.90244	0	0	10.9698	3.6986
Bus 32	0.58693	-0.50466	0	0	0.15761	1.8493

Under heavy load condition, the weakest bus is bus17 with voltage 0.58128 pu followed by bus 18 with voltage 0.58496 pu and bus 32 with voltage 0.58693.

The eigenvalue of each bus is calculated and listed in Table 4.

melatsharafany89@gmail.com

Table (4): Eigenvalue of weakest buses at maximum load

Bus	Eigenvalue
Bus 32	23
Bus 17	182
Bus 18	186

By using the Q-V curve technique, the system becomes unstable at heavy load condition because one of the eigenvalues has a negative sign. The eigenvalue 16 that related to bus 17 is equal to -0.77524.

4.2 Impact of a SPVG on static voltage stability

The best location for SPVG is the weakest bus or nearest bus to the weakest bus [7]. From section 4.1, it is concluded that the weakest bus is bus 32. The impact of SPVG on static voltage stability is presented at nominal and heavy load conditions. Active power reference of the SPVG is assumed to be 100Mw, the voltage reference is 1 pu, both inverter response times (T_p, T_q) are 0.015 sec and voltage PI controller gains, k_v and k_i, are 0.08686 and 50.9005 respectively. These parameters have been selected after many traials.

4.2.1 SPVG connected to weakest bus

The SPVG PV-model is added at bus 32 as the weakest bus to enhance the voltage stability of the system. The power flow technique is applied to the system and the results are listed in

Table (5.

Table (5): Power flow results with SPVG at bus 32

Bus	V p.u.	Phase rad.	P_g p.u.	Q_g p.u.	P_L p.u.	Q_L p.u.
Bus 17	0.95707	-0.15829	0	0	2.338	0.84
Bus 18	0.95735	-0.16766	0	0	5.22	1.76
Bus 32	1	-0.0581	1	1.9926	0.075	0.88

After adding SPVG PV-model at bus 32, the buses voltages are increased; bus 32 from 0.93491 pu to 1 pu; bus 17 from 0.94407 pu to 0.95707 pu and bus 18 from 0.944752 pu to 0.95735 pu.

Under heavy load, the CPF is applied to the system and the results are listed in Table 6.

Table (6): CPF results with SPVG at bus 32

Bus	V p.u.	Phase rad.	P_g p.u.	Q_g p.u.	P_L p.u.	Q_L p.u.
Bus 17	0.64895	-0.80725	0	0	5.4619	1.9624
Bus 18	0.6495	-0.85792	0	0	12.1947	4.1116
Bus 32	1	-0.48331	1	12.8486	0.17521	2.0558

Also at the heavy load condition, buses voltages are increased after adding SPVG PV-model to the weakest bus. The voltage of bus 17, bus 18 and bus 32 are increased from 0.58128 pu to 0.64895 pu, 0.58496 pu to 0.6495 pu and 0.58693 pu to 1 pu, resectively.

The Q-V curve technique is applied to the system at nominal and heavy load conditions. The results demonstrated that the system becomes unstable at heavy load condition since one of the eigenvalues has a negative sign. The eigenvalue 15 that related to bus 35 is -0.96816.

melatsharafany89@gmail.com

The results showed that by adding SPVG PV-model to bus 32, the voltage stability is enhanced at nominal load condition. However, the system becomes unstable at heavy load condition.

4.2.2 SPVG connected at bus 31

The nearest bus to weakest bus is bus 31 and bus 33. In this section, SPVG PV-model is connected and tested at bus 31 at nominal and heavy load conditions. The power flow technique is applied to the system and the results are listed in Table 7.

Table (7): Power flow result with SPVG at bus 31

Bus	V p.u.	Phase rad.	P_g p.u.	Q_g p.u.	P_L p.u.	Q_L p.u.
Bus 17	0.97256	-0.15492	0	0	2.338	0.84
Bus 18	0.97222	-0.16402	0	0	5.22	1.76
Bus 32	0.97482	-0.0794	0	0	0.075	0.88

By adding SPVG at bus 31 instead of bus 32, the voltage of bus 17 and voltage bus 18 are increased while the voltage of bus 32 is decreased.

Under heavy load condition, the CPF is applied to the system and the results are listed in Table 8.

Table (8): CPF results with SPVG PV-model at bus 31

Bus	V p.u.	Phase rad.	P_g p.u.	Q_g p.u.	P_L p.u.	Q_L p.u.
Bus 17	0.90591	-0.42157	0	0	4.6273	1.6625
Bus 18	0.90281	-0.4431	0	0	10.3314	3.4834
Bus 32	0.9363	-0.2762	0	0	0.14844	1.7417

The results showed that there is an increase of voltage of bus 17 and voltage of bus 18 after adding SPVG at bus 31.

By using the Q-V curve technique, the system is stable under nominal and heavy load conditions because all eigenvalues have positive sign. It is shown that SPVG at bus 31 provides better performance compared to bus 32 in improving the voltage of buses and stability of the system.

4.2.3 SPVG connected at bus 33

Bus 33 is also the nearest bus to the weakest bus. SPVG is connected at bus 33. The power flow technique is applied to the system and the results are listed in Table 9.

Table (9): Power flow result with SPVG at bus 33

Bus	V p.u.	Phase rad.	P_g p.u.	Q_g p.u.	P_L p.u.	Q_L p.u.
Bus 17	0.96548	-1.56	0	0	2.338	0.84
Bus 18	0.96557	-0.16544	0	0	5.22	1.76
Bus 32	0.97278	-0.07825	0	0	0.075	0.88

By adding SPVG at bus 33 instead of bus 31, the voltage of buses are decreased and the total losses is increased.

Under heavy load condition, the CPF is applied to the system and the results are listed in Table 10.

melatsharafany89@gmail.com

Table (10): CPF results with SPVG at bus 33

Bus	V p.u.	Phase rad.	P_g p.u.	Q_g p.u.	P_L p.u.	Q_L p.u.
Bus 17	0.87699	-0.44773	0	0	4.7003	1.6887
Bus 18	0.87529	-0.47085	0	0	10.4941	3.5383
Bus 32	0.93264	-0.29428	0	0	0.15078	1.7691

The reslts showed that under heavy load condition, the voltage of buses are decreased compared to the case at which SPVG is connected at bus 31.

By using the Q-V curve technique, the results showed that the system is stable under nominal and heavy load conditions.

5. CONCLUSION

The effect of a SPVG on voltage stability of the system using three static analysis was assessed in this paper. New England 39-bus system was used as the test system. The weakest buses were obtained using static techinques at nominal and heavy load conditions based on the voltage magnitude and eigenvalue of each bus. The results showed that bus 32 is the weakest bus. The SPVG was tested at different locations to improve the voltage staility of the system. The results obtained revealed that the voltage stability improved by adding SPVG to the system. Also, the results demonstrated that connecting SPVG to the nearest bus to the weakest bus provides better results than when it connected to the weakest bus in terms of the voltage of buses and system stability. Therefore, bus 31 was identified as the optimum location of SPVG for the test system.

melatsharafany89@gmail.com

APPENDIX A

A single line diagram of the New England 39-bus system

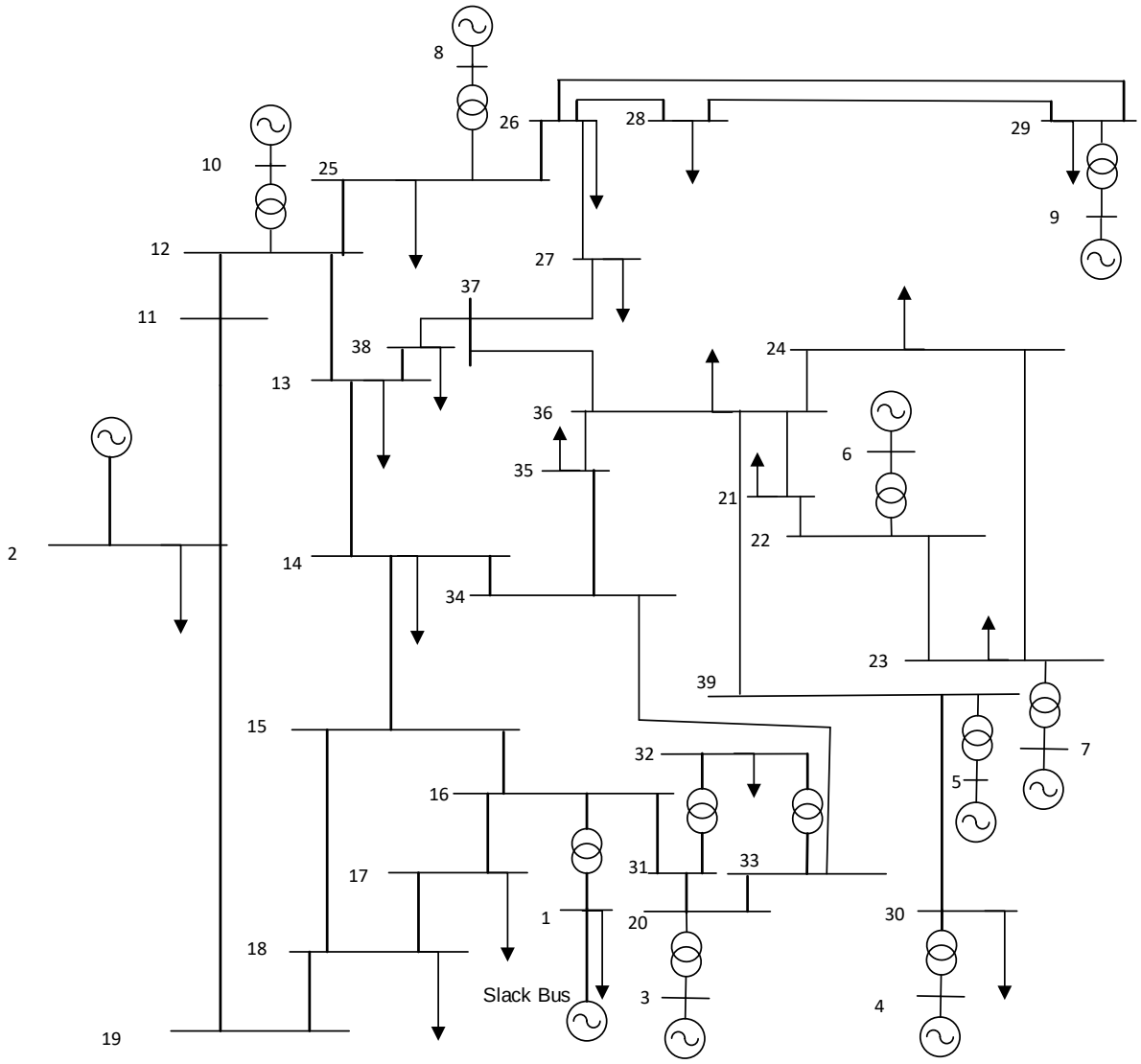

REFERENCES

Uncategorized References

A. D. Vasquez, & T. Sousa, U. (2017). *Voltage Stability Analysis of Power Systems using the Continuation Method* Paper presented at the THE 12th LATIN-AMERICAN CONGRESS ON ELECTRICITY GENERATION AND TRANSMISSION, Mar del Plata, Argentina.

A. Elrheem E.A. Mostafa, Naglaa K. Bahgaat, Mohamed Ebrahim El sayed, & Othman4, a. E.-S. A. (2017). Voltage Stability for a Photovoltaic System Connected to Grid by Using Genetic Algorithm Technique. *International Journal of Grid and Distributed Computing, 10*(4), 33-42.

Chang, G., Yuwei, S., Chengqing, Y., Xinping, Y., Yang, W., & Qizhen, J. (2015, 22-25 Nov. 2015). *Research on Power Load Flow Calculation for Photovoltaic-Ship Power System Based on PSAT.* Paper presented at the 2015 International Conference on Renewable Energy Research and Applications (ICRERA).

Ghaffarianfar, M., & Hajizadeh, A. (2018). Voltage Stability of Low-Voltage Distribution Grid with High Penetration of Photovoltaic Power Units. *Energies, 11*(8).

melatsharafany89@gmail.com

Hassan, L., Moghavvemi, M., & Almurib, H. F. (2012). Modeling UPFC into Multi-Machine Power Systems. *Arabian Journal for Science and Engineering, 37*(6), 1613-1624. doi: 10.1007/s13369-012-0273-7

Hassan, L. H. (2017). *Impact of a PV Controller on Stability of Renewable Energy Based Large Distribution Systems* Paper presented at the 3rd International conference on artificial intelligence, computer, electrical and electronics engineering (ICACEEE), Kuala Lmpur.

Hassan, L. H., Mohamed, H. A., Moghavvemi, M., & Yang, S. (2008, 7- 9 March). *Contingency Monitoring and Voltage Collapse Estimation for Iraqi National Super Grid System.* Paper presented at the The 4th International Colloquium on Signal Processing and its Applications (CSPA) 2008 Kuala Lumpur.

Heetun, K. Z., Abdel Aleem, S. H. E., & Zobaa, A. F. (2016). Voltage Stability Analysis of Grid-Connected Wind Farms With FACTS: Static and Dynamic Analysis. *Energy and Policy Research, 3*(1), 1-12. doi: 10.1080/23317000.2015.1128369

Kundur, P. (1994). *Power System Stability And Control*: McGraw-Hill.

Kundur, P., Paserba, J., Ajjarapu, V., Andersson, G., Bose, A., Canizares, C., . . . Vittal, V. (2004). Definition and Classification of Power System Stability IEEE/CIGRE Joint Task Force on Stability Terms And Definitions. *IEEE Transactions on Power Systems, 19*(3), 1387-1401.

Munkhchuluun, E., & Meegahapola, L. (2017, 4-7 Dec. 2017). *Impact of The Solar Photovoltaic (PV) Generation on Long-Term Voltage Stability of a Power Network.* Paper presented at the 2017 IEEE Innovative Smart Grid Technologies - Asia (ISGT-Asia).

Nikpour, N. (2016). *Dynamic and Static Voltage Stability Analysis of Distribution Systems in the Presence of Distributed Generation.* The university of British Columbia

Noel, D., Sozinho, F., Wilson, D., & Hatipoglu, K. (2016, 30 March-3 April 2016). *Analysis of Large Scale Photovoltaic Power System Integration into the Existing Utility Grid Using PSAT.* Paper presented at the SoutheastCon 2016.

Omole, A. (2010). *Voltage Stability Impact of Grid-Tied Photovoltaic Systems Utilizing Dynamic Reactive Power Control.* Retrieved from https://ui.adsabs.harvard.edu/abs/2010PhDT.....46O

Refaat, S. S., Abu-Rub, H., Sanfilippo, A. P., & Mohamed, A. (2018). Impact of Grid-Tied Large-Scale Photovoltaic System on Dynamic Voltage Stability of Electric Power Grids. *IET Renewable Power Generation, 12*(2), 157-164. Retrieved from: https://digital-library.theiet.org/content/journals/10.1049/iet-rpg.2017.0219

Sinder, R. L., Assis, T. M. L., & Taranto, G. N. (2019). Impact of Photovoltaic Systems on Voltage Stability in Islanded Distribution Networks. *The Journal of Engineering, 2019*(18), 5023-5027.

Suampun, W. (2016). Voltage Stability Analysis of Grid-connected Photovoltaic Power Systems Using CPFLOW. *Procedia Computer Science, 86*, 301-304. doi: https://doi.org/10.1016/j.procs.2016.05.082

Tamimi, B., Canizares, C., & Bhattacharya, K. (2013). System Stability Impact of Large-Scale and Distributed Solar Photovoltaic Generation: The Case of Ontario, Canada. *IEEE Transactions on Sustainable Energy, 4*(3), 680-688. doi: 10.1109/tste.2012.2235151

Tamimi, B., Cañizares, C., & Bhattacharya, K. (2011, 24-28 July 2011). *Modeling and Performance Analysis of Large Solar Photo-Voltaic Generation on Voltage Stability and Inter-Area Oscillations.* Paper presented at the 2011 IEEE Power and Energy Society General Meeting.

Vahid-Pakdel, M. J., Seyedi, H., & Mohammadi-Ivatloo, B. (2018). Enhancement of Power System Voltage Stability in Multi-Carrier Energy Systems. *International Journal of Electrical Power & Energy Systems, 99*, 344-354. doi: https://doi.org/10.1016/j.ijepes.2018.01.026

Wang, D., Yuan, X., Zhao, M., & Qian, Y. (2017). Impact of Large-Scale Photovoltaic Generation Integration Structure on Static Voltage Stability in China's Qinghai Province Network. *The Journal of Engineering, 2017*(13), 671-675.

Wang, Y.-B., Wu, C.-S., Liao, H., & Xu, H.-H. (2008, 21-24 April 2008). *Steady-State Model and Power Flow Analysis of Grid-Connected Photovoltaic Power System.* Paper presented at the 2008 IEEE International Conference on Industrial Technology.

Xue, Y., Manjrekar, M., Lin, C., Tamayo, M., & Jiang, J. N. (2011, 24-28 July 2011). *Voltage Stability and Sensitivity Analysis of Grid-Connected Photovoltaic Systems.* Paper presented at the 2011 IEEE Power and Energy Society General Meeting.

melatsharafany89@gmail.com